Interaction of cholesterol-like molecules in polyunsaturated phosphatidylcholine lipid bilayers as revealed by a self-consistent field theory

F. A. M. Leermakers[1] and A. L. Rabinovich[2]
[1]*Laboratory of Physical Chemistry and Colloid Science, Wageningen University, Dreijenplein 6, 6703 HB Wageningen, the Netherlands*
[2]*Institute of Biology, Karelian Research Centre, Russian Academy of Sciences, Pushkinskaya Street 11, R-185910 Petrozavodsk, Russia*
(Received 24 May 2007; revised manuscript received 31 July 2007; published 10 September 2007)

Cholesterol is one of the most abundant components in biological membranes. In this paper we apply a detailed state-of-the-art self-consistent field (SCF) theory to predict the influence of cholesterol-look-alikes in the bilayer composed of 1-stearoyl-2-docosahexaenoyl-*sn*-glycero-3-phosphatidylcholine (18:0/22:6ω3*cis* PC) lipids with a polyunsaturated 22:6 and a fully saturated 18:0 tail. The cholesterol-like molecule is composed of a hydroxyl group, a rigid chain fragment with length n segments and a branched semiflexible moiety with methylene side groups. We vary both the length of the rigid fragment in the cholesterol-look-alikes and their mole fraction in the tensionless bilayers. We find that these additives significantly increase the order of the saturated tails, but influence the conformational properties of the unsaturated tail much less. With increasing loading the bilayer thickness and the area available per PC head group increase. The hydroxyl group anchors close to the membrane-water interface, but with increasing loading the distribution of this polar group widens. The orientational order of the rigid part is high and we conclude that the cholesterol has significant mobility in the normal direction in the hydrophobic region of the bilayer indicating that one singly hydroxyl group is giving only a weak anchoring to the water-interface. Cholesterol-look-alikes increase the fluctuation of the tail ends and decrease the interdigitation of the tails. Several of our predictions correspond to molecular dynamics (MD) simulation results, but there are also important differences. Most notably the cholesterol-look-alikes can visit the membrane symmetry-plane more easily in SCF than in MD. Possible reasons for this are discussed.

DOI: 10.1103/PhysRevE.76.031904 PACS number(s): 82.39.Wj, 87.14.Cc

I. INTRODUCTION

The significance of cholesterol in biological membranes has been known for a long time. A large number of experimental and theoretical studies has been devoted to unravel the modes of action of this molecule (for reviews see, e.g., Refs. [1–5]). Cholesterol is known both to order the lipids [6–9] and to suppress the gel-to-liquid phase transition [7,10–18], showing that these trends can indeed be decoupled. Cholesterol (i.e., 5-cholesten-3β-ol) includes a tetracyclic fused ring skeleton which renders the molecule to be planar and rather stiff because the rings of cholesterol are fused in the trans configuration [1,13,19]. On one of the extremities there exists a hydroxyl group (3β-OH) which is slightly hydrophilic. This group prefers to be hydrated and as a result the cholesterol molecule is oriented along the membrane normal. The hydrocarbon tails of the lipid molecule will align themselves with the rigid part of the cholesterol molecule [20] and therefore the segment order parameter appears to be higher in the presence of significant amounts of cholesterol; these considerations are in line with the available experimental data [6–9]. The rigid part of the cholesterol molecule is not of the same length as the acyl chains of the most widespread natural lipids. However, the size mismatch is compensated, to a great extent, by a short flexible (iso-octyl) chain attached to the other extreme of the rigid backbone. The 3β-OH group of cholesterol, the two side methyl groups CH_3 (which are disposed between the first and second rings, and the third and fourth rings) and the side iso-octyl chain are all located on the same side of the ring skeleton. Thus, the three-dimensional structure of cholesterol represents the so-called "β configuration" [1,21]. Including the flexible fragment (chain) the cholesterol is approximately of the same size as a typical acyl chain of $\sim$16 carbons. According to Ref. [22], the best match between the effective length of the cholesterol molecule and the mean hydrophobic thickness of the phospholipid bilayers is obtained with the 17:0/17:0 PC molecule. As a result cholesterol packs conveniently in between the lipid molecules and the mixing with lipids can persist up to high molar ratios. For example, it has been revealed by the ^{13}C NMR study of nonperturbed multilamellar model membranes formed by egg yolk phosphatidylcholine (PC) [23], that cholesterol is placed in such a position that it is not readily exposed to the solvent: the hydrophobic steroid rings are oriented parallel to the membrane phospholipids, the hydroxyl group is in close vicinity to the phospholipid ester carbonyl groups and the iso-octyl side chain is deeply buried in the centre of the membrane [23].

The cholesterol orientation characterized by small tilt angles with the bilayer normal were measured by solid state ^{2}H NMR in 18:0/18:1ω9cis PC, 18:0/20:4ω6cis PC, 18:0/22:6ω3cis PC, and 20:4ω6cis/20:4ω6cis PC bilayers [24]. Similar result was obtained for cholesterol orientation in 18:0/22:6ω3cis PC and 22:6ω6cis/22:6ω6cis PC bilayers using low- and wide-angle x-ray diffraction [25]. In relevant biological systems the fraction of cholesterol can be as high as 50 mol % [26–32]. For such high molar ratios it will be obvious that with increasing loading the bilayers will increase their thickness. More correctly, cholesterol can either increase or decrease the width of the bilayer depending on the physical state and chain length of the lipid before the

introduction of cholesterol [33]. According to x-ray diffraction investigation [33], for saturated PCs containing 12–16 carbons per chain, cholesterol increases the width of the bilayer as it removes the chain tilt from gel state lipids or increases the *trans* conformations of the chains for liquid crystalline lipids (in accordance with Refs. [6–9]). The results of the small-angle neutron scattering from aqueous multilammellar 14:0/14:0 PC lipid bilayers [34] indicate that the effect of small amounts of cholesterol, $\leqslant 3$ mol %, is a softening (reduced bending rigidity) of the bilayers in the gel-liquid phase transition region, whereas cholesterol contents above this range lead to the well-known effect of rigidification. However, cholesterol reduces the width of 18 carbon chain bilayers below the phase transition temperature as the long phospholipid chains must deform or kink to accommodate the significantly shorter cholesterol molecule [33].

As the hydrophilic "head" of the cholesterol is rather small it does not directly add much to the stopping mechanism that regulates the membrane thickness. The crowding of the PC head groups of the lipid molecules on the other hand gives one of the main stopping mechanism that determines the membrane thickness (above the gel-liquid crystalline phase transition temperature T_m). Another stopping mechanism for the growth of the membrane thickness is the finite extensibility of the lipid tails. The area available per PC containing lipid molecule (total area divided by the number of PC lipids) is significantly perturbed when a sufficient number of cholesterol molecules are inserted [35–37]. On first sight we may anticipate that this quantity increases with increasing loading simply because the hydrophobic volume of the lipid/cholesterol mixture increases. According to Refs. [35–37], however, the partial specific area (the area under the PC chain) available per lipid molecule (16:0/16:0 PC was described) decreases with increasing cholesterol content because of the condensing effect of cholesterol and the effect on the thickness of the membrane core. Other, perhaps more subtle responses may be discussed, e.g., the level of chain interdigitation of tails into opposite sides of the bilayer, the fluctuations of the tail ends and the head group conformation.

Cholesterol is suggested to form "condensed complexes" [38,39] with phospholipids in the plasma membrane. Cholesterol has pronounced effects on the dynamical properties of the bilayers as well [40–43]. For example, ^{2}H NMR relaxation study of 14:0/14:0 PC and 14:0/14:0 PC: cholesterol bilayers dynamics was performed [42], and collective motions are found to be less predominant in the case of 14:0/14:0 PC: cholesterol than for pure 14:0/14:0 PC, which may indicate an increased dynamical rigidity of lipid bilayers containing cholesterol versus pure lipid systems [42]. ^{13}C solid-state NMR spectroscopy measurements [43] indicate that the presence of cholesterol significantly decreases the rate and/or amplitude of both the high and low frequency motions in the 14:0/14:0 PC: cholesterol bilayers [43]. At the same time the relatively high rates of lateral and rotational diffusion characteristic for fluid phospholipid bilayers with cholesterol are maintained [15,44]. Obviously, the "condensed complexes" themselves may have structures that fluctuate rapidly over a range of conformations and can have a repulsive interaction with other phospholipids, leading to immiscibility [38]. This goes along with the suppression of the gel-to-liquid phase transition [7,10–18]. Whether this effect can be traced back to the increased head group area available for the PC heads, the modifications with respect to the tail interdigitation, the increased orientational order of the acyl tails, the possible variations in the packing densities of the molecules, are largely unknown.

We will employ a detailed self-consistent field (SCF) model to study the influence of cholesterol-look-alikes on the membrane properties of one particular bilayer in order to search for some answers to these questions. Indeed we will obtain only information on the static properties of the problem and this will leave the dynamical issues mentioned above largely unanswered. For dynamical information one needs to turn to simulation technique such as molecular dynamics (MD) [45–49].

Several years ago we reported on the membrane properties of PC bilayers in a set of papers [50–52] where the detailed SCF results were compared to those of MD. The conclusion of this study was that the SCF results were following the (exact) MD results in a remarkable semiquantitative way. This is significant because the SCF model is many orders of magnitude more efficient in terms of the use of CPU. The success of our previous investigations gives us confidence that the parameters used in the SCF modeling are reasonable. Below we will introduce cholesterol-look-alikes which we will admix with the model bilayer composed of 1-stearoyl-2-docosahexaenoyl-*sn*-glycero-3-PC (18:0/22:6ω3*cis* PC) bilayers. At this stage we stress that the molecular model for the cholesterol molecules is still very primitive. The target is to mimic the main characteristics of this type of molecules, having a polar group, a rigid moiety and a flexible tail. The label "cholesterol look-alike" is used for ease of reference to the inclusions. In this primitive model no new interaction parameters are needed and we will refer to our previous paper [52] for all details about our model and the parameters used. We also refer to this paper for a short overview of complementary SCF calculations that are available in the literature; we will not repeat this overview here. Below we will only outline our method and mention the basic approximations.

It should be preliminary mentioned that the polyunsaturated (PU) lipid bilayer was chosen for our study because PU chains of lipids, especially 22:6ω3*cis*, are of great importance in structure and functioning of natural membranes [53,54]. The objects of our previous investigations [50–52] were several PU lipid bilayers as well. In the last few years, a considerable quantity of reviews [53–61] have been devoted to various aspects of this problem. It is known that cholesterol has a low affinity for highly unsaturated phospholipids in comparison with the saturated ones [1,5,62], but full understanding of the effects of lipid unsaturation as well as cholesterol on various physical properties of membranes at the molecular level is not yet achieved.

The remainder of this paper is as follows. First we will give a short introduction in the SCF modeling technique. Then we will introduce the cholesterol-look-alikes(s). In the results section we will concentrate mostly on the comparison of the pure lipid bilayer with the bilayer with a mole fraction of $x=0.4$ of inclusions. The advantage of the SCF method is

that one can easily generate trends. These trends should be trusted more than the absolute numbers. We will discuss various membrane characteristics as a function of the fraction of cholesterol in the bilayer. As the exact structure of the cholesterol-like inclusions is not accounted for, we will discuss the effect of the length of the rigid fragment in an attempt to generate generic information for a class of inclusions.

II. SCF THEORY

Unlike in simulation techniques, where the conformation of each molecule at each point in time depends on the actual surrounding, the ansatz in self-consistent field (SCF) theory is to assume that there exists some average surrounding for a molecule in a particular conformation/position in the system. Instead of a strongly coupled problem in which all molecules mutually depend on each other, in the SCF model one obtains a decoupled problem of a single chain/molecule in an external field. Usually one refers to the external fields as self-consistent potentials because the potentials are not fixed, but adjusted iteratively to account for the average distributions in the system. Therefore there are two conjugated distributions in the system for each type of segment A. First there are the concentration profiles. Typically one used dimensionless concentrations, i.e., volume fractions $\varphi_A(\mathbf{r})$ by normalizing the concentrations by the segment volume. Complementary to these concentrations are the self-consistent potentials $u_A(\mathbf{r})$. At the basis is a free energy which is the characteristic function in the $(\{n\},V,T)$ ensemble is in the SCF theory expressed in a complicated way, namely, as a functional $F([\{\varphi\}_A,\{u\}_A,u']\mathbf{(r)})$. Here the square brackets indicate that this free energy is a functional of the properties mentioned, the curly brackets point to the fact that all volume fractions and all potentials, i.e., for all segment types, are used. This Helmholtz energy contains four terms

$$F = -kT \ln Q[\{u\}] - \sum_A \sum_{\mathbf{r}} u_A(\mathbf{r})\varphi_A(\mathbf{r}) + F^{\text{int}}[\{\varphi\}] + \sum_{\mathbf{r}} u'(\mathbf{r})\left(\sum_A \varphi_A(\mathbf{r}) - 1\right), \tag{1}$$

where the summation over all coordinates points to the fact that a lattice model is used (more details are given below). The first two terms of Eq. (1) give the (observable) overall entropy (conformational and translational) of the molecular entities in the system. The third term accounts for all the interactions in the system. This term can be uniquely calculated when the volume fractions are known. The final term in Eq. (1) shows that there is a (compressibility) constraint that the sum over all volume fractions locally add up to unity. The Lagrange parameter $u'(\mathbf{r})$ is one of the parameters of the free energy functional. The free energy functional of Eq. (1) is optimized with respect to its variables

$$\frac{\delta F}{\delta \varphi_A(\mathbf{r})} = 0 \Rightarrow \frac{\delta F^{\text{int}}}{\delta \varphi_A(\mathbf{r})} - u_A(\mathbf{r}) = 0, \tag{2a}$$

$$\frac{\delta F}{\delta u_A(\mathbf{r})} = 0 \Rightarrow \frac{-kT\delta \ln Q[\{u\}]}{\delta u_A(\mathbf{r})} - \varphi_A(\mathbf{r}) = 0, \tag{2b}$$

$$\frac{\delta F}{\delta u'(\mathbf{r})} = 0 \Rightarrow \sum_A \varphi_A(\mathbf{r}) - 1 = 0, \tag{2c}$$

where Eqs. (2a) and (2b) are needed for all segment types and Eqs. (2a)–(2c) apply to all coordinates. It turns out that the free energy features a minimum with respect to the volume fraction, but a maximum with respect to the segment potential. Formally, the physically realistic solutions obeys to a saddle point of the free energy. Equations (2a)–(2c) specify how to find a physical solution of the free energy (1). When such a solution is available, we can evaluate the free energy and from subsequent differentiations all other thermodynamic and mechanical observables (such as the membrane tension) follows. To make these equations operational we have to mention what terms are included in the interaction part of the free energy and how the partition function is evaluated from the potentials. In the mean field approximation the overall partition function can be factorized in terms of single-chain partition functions $\{q\}_i$

$$Q = \sum_i \frac{q_i^{n_i}}{n_i!}, \tag{3}$$

where i refers to a ranking number of the molecule types.

According to Eq. (2), the classical SCF formalism can schematically be expressed as

$$\varphi[u(\mathbf{r})] \Leftrightarrow u[\varphi(\mathbf{r})] \tag{4}$$

which must be evaluated, while obeying the compressibility constraint [Eq. (2c)]. This problem is solved on a discrete space (lattice). More specifically, we use the discretization scheme of Scheutjens and Fleer [63–68]. Equation (4) expresses on the left-hand side that the volume fraction profiles (of all components in the system) follow (uniquely) from the potential profiles [as follows from Eq. (2b)]. Of course, to implement this step one has to define a chain-model (for details, see Ref. [52]). With this chain model one can evaluate the single chain partition functions. Here we will use a rotational isomeric state (RIS) scheme which assures the excluded-volume correlations of any sequence of four segments. For the acyl chain the local trans-configuration is lower in energy than the gauche conformations by $0.8\ k_BT$. Excluded-volume correlations of segments further apart are neglected which means that the chain can fold back on previously visited sites. This approximation is acceptable because intrachain excluded-volume correlations are also not fully obeyed. As a result we have a reasonable balance between intrachain and interchain excluded-volume correlations. One of the tails in the lipid molecule has unsaturated bonds. We approximate the modeling of such bond by forcing a local gauche conformation. This is done by favoring (*ad hoc*) the gauche conformation by $10k_BT$ over the local *trans* configuration. This allows us to use the RIS scheme without extra complications. As we will discuss shortly the cholesterol molecule has a rigid fragment. This is implemented by favoring the trans over gauche by (again *ad hoc*)

$10k_BT$ in the rigid part of the molecule. The lipid molecule is modeled in great detail. The RIS scheme has been generalized such that one can efficiently account for the conformational degrees of freedom of the nonlinear molecules (the glycerol moiety has a saturated alkyl tail 18:0 on the *sn*-1, a polyunsaturated chain 22:6 on the *sn*-2 position and a phosphatidylcholine moiety which is zwitterionic on the *sn*-3 position). Within this scheme we generate all possible and allowed conformations of the molecules. For each conformation c, the potential energy u_c is computed and the statistical weight of this conformation is proportional to $\exp(-u_c/k_BT)$. On top of this, the statistical weight of a given conformation depends on the direction of its bonds. If in the system there are locally many bonds going in a particular direction, one is necessary to give a chain which has many bonds in line with this particular direction (director) some extra statistical weight. Chains that go against the global order do not obtain this extra weight. This results in the so-called SCAF model which is essential when the model features densely packed chains [65]. This SCAF model also features the so-called gel-to-liquid phase transition, but we will choose the conditions in this paper such that we will remain in the liquid state. The volume fraction profiles are found after normalizing the statistical weights of the full set of conformations. In passing we mention that there exists an extremely efficient propagator formalism to compute in the RIS formalism the statistical weight of all possible conformations. In this formalism the number of computations grow only linearly with the number of segments in the molecule.

The right-hand-side of Eq. (4) expresses the dependence of the potentials on the volume fraction profiles and is a schematic for Eq. (2a). In the free energy F^{int} and thus also in the segment potentials we account for three types of contributions. First there is the potential field which is needed to obey the compressibility relation, i.e., the Lagrange term $u'(\mathbf{r})$ in each coordinate $\mathbf{r}$ [below we will use one gradient, that is in the z direction, perpendicular to the membrane surface, i.e., we perform "one-dimensional" calculations; one consequence of this is that the free energy given in Eq. (1) is now typically expressed per unit area]. In the summation over all segment types in Eq. (2c) the summation includes the solvent molecules, the ions, and the vacancies (see below). The second contribution to the segment potentials is a term which accounts for the local nearest-neighbor interactions. To approximate the number of contacts we use the volume fraction profiles (Bragg-Williams approximation) where we account for the fact that one segment not only interacts with other segments that are at the same z coordinate, but also with segments in neighboring coordinates, i.e., $z-1$ and $z+1$. The interactions are parametrized by Flory-Huggins χ parameters, which (for incompressible systems) have nonzero values for all unlike A-B contacts. For repulsive interactions $\chi_{AB}>0$ and for attraction $\chi_{AB}<0$. The full set of interaction parameters has been published before [52]. It suffices here to mention that the hydrocarbon-water interaction is taken sufficiently repulsive such that the tails have the strong tendency to escape from the water phase. This drives the self-assembly. In the phosphatidylcholine head group there is a positive and a negative charge and the parameters are chosen such that the head group prefers to be solvated with water. In addition, we have monovalent salt ions in our system. The concentration is fixed to a volume fraction in the bulk (far from the bilayer) to $\varphi_s=0.01$. As a result, the third contribution to the segment potential is the usual electrostatic term, exactly equivalent to the one used in the Poisson-Boltzmann (PB) theory. In fact one can classify our method as a very elaborate PB theory in which the ions have volume and besides charged units there are chains with polar and apolar moieties. The electrostatic potential is found by solving the Poisson equation [69,70]. The charge density profile follows trivially from the volume fraction profiles. The dielectric permittivity profile is computed from a volume fraction weighted average. This means that for each segment type we need to provide the system with such values. For example, we take for the relative dielectric constants for the hydrocarbon units $\varepsilon_{rC}=2$ and for water $\varepsilon_{rW}=80$.

The self-consistent solution of Eq. (4) has the property that the potentials that are needed to calculate the volume fractions [left-hand-side of Eq. (4)] are exactly found back from the calculations of the potentials [right-hand-side of Eq. (4)] wherein the volume fractions are the input. In addition the volume fractions of the SCF solution obey the incompressibility constraint of Eq. (2c). Such a solution is found routinely by an iterative procedure with high precision and extremely little CPU time (order seconds on a desktop PC).

As the lipid molecules are very apolar, one finds virtually zero lipids in the water phase (note that there are no constraints imposed on any of the molecules). Sufficiently far from the bilayer we therefore have effectively an aqueous solution with 1:1 electrolyte. We allow for some free volume (vacant sites) and we use a rather primitive water model which allows for the presence of clusters of water molecules which are mutually in equilibrium with each other. Details of the water model can also be found in our previous publication [52]. The interest in using the water-cluster model is that it will lead to very low amounts of water in the membrane core. The free volume is needed in the model to prevent direct crystallization of the tails in the membrane (that is, it prevents for the present set of parameters the formation of the gel-phase).

Cholesterol is modeled as a sequence of (united) segments with the sequence $(O)_1(X)_n(C)1[C](C)_4[C](C)_1$. In this chain of segments the X refers to the rigid part where the local trans conformer is strongly favored over the gauche conformers. The $[C]$ unit is not part of the main chain but is a side group. Chemically the X segment is identical to the C segment (which is identical to the hydrocarbon C in the lipid molecule). Only the O, which stands for the OH group is hydrophilic and the parameters are the same as for the O in the glycerol fragment of the lipid molecule. Of course this linear molecule is just a caricature of the real cholesterol molecule. Most importantly, the volume of the rigid fragment is not accurately accounted for. However, the main characteristics, that is a rigid backbone and a flexible tail, follows that found in cholesterol and therefore we believe that this cholesterol-look-alike will give qualitative insight in the behavior of real cholesterol in bilayers. The parameter n, which represents the length of the rigid fragment, is kept as a variable in our study. From the molecular structure of cholesterol we may choose $n=9$ to be representative for cholesterol. Be-

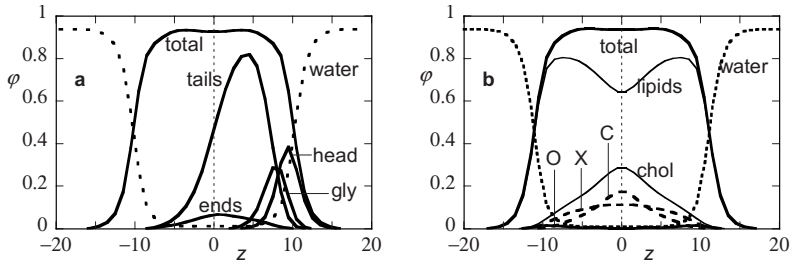

FIG. 1. (a) Volume fraction profile across a tensionless, cholesterol-free bilayer composed of 18:0-22:6-PC lipids. The total symmetric volume fraction profile of the water (dashed line) and the lipids are given. The profile of the overall segments of the head group, the glycerol moiety, the two tails and the tail ends are given for those molecules that have the phosphate on the right side of the bilayer. The symmetry plane at $z=0$ is dotted. Not shown are the distributions of the 1:1 electrolyte and the free volume. (b) Volume fraction profile across a tensionless bilayer composed of $x=0.4$ mol fraction of cholesterol ($n=9$). The total density (lipids plus cholesterol), the individual profiles of the lipids and cholesterol (chol) are given by thin lines, water is dotted and the three contributions to the cholesterol profile (O, X, and C) are indicated separately. The O profile has a very broad peak (difficult to see because of the low density). The partial profiles for the fragments of the lipid molecule are qualitatively similar to the ones shown in (a). The z coordinate is in units l of the segment length. Comparison with molecular dynamics (MD) suggests a value of $l=0.25$ nm for this conversion factor. The volume fractions should not be confused by the mass distribution. This complicates the direct comparison with MD.

low we will also discuss results for a shorter $n=6$ molecule and a longer one $n=12$.

The self-consistent field solution of Eq. (1) allows us to obtain very accurate value for the structural and thermodynamic quantities. In essence we solve the mean field problem exactly. Below we will be interested in flat bilayers. In this case the mean-field averaging is done in planes parallel to the membrane surface and our coordinate of interest is the z direction which is perpendicular to the membrane surface. We stress that the lipids have no positional constraints on any of our molecules. These are not needed because we realistically account for the driving forces for self-assembly as well as all the possible stopping mechanisms. The most relevant thermodynamic quantity that is computed is the membrane tension γ. Freely floating bilayers can use the membrane area as an adjustable parameter. In this situation the equilibrium is such that the membrane tension vanishes, i.e., $\gamma=0$. Below we present results for which the absolute value of the surface tension is less than $10^{-5}k_BT/l^2$ (approximately 10^{-5} mN/m). For computation reasons it is convenient to force the bilayers to be symmetric with respect to the symmetry plane in the center of the core of the bilayer. For flat equilibrium membranes this is not an extra approximation.

III. RESULTS AND DISCUSSION

Let us first compare the volume fraction profiles across the tensionless cholesterol-free bilayers with corresponding ones with a molar fraction of $x=0.4$ for the cholesterol-look-alike $n=9$. In Fig. 1(a) we collected the results of the cholesterol-free bilayer. In this figure we show the symmetric profile of the lipids and water. We see that there is very little water in the core of the bilayer and that the packing density of the lipids in the core is virtually constant. There is a small depression of the density in the core which is attributed to the fact that in the core the chain order is less than just below the glycerol backbone region. The free volume profile (not shown) shows some small variations throughout the bilayer. More importantly the amount of free volume in the bilayer is slightly larger than in the water phase. In the same figure we present the distribution of the head group units, the cholesterol as well as the tails for those chains that have the head group on positive z coordinates (the $z=0$ is taken at the symmetry plane). The orientation of the head group (not shown; defined by the vector from the phosphate to the choline group) is almost parallel with the membrane surface that is consistent with the experimental data [71–75]. There are several reasons for this head group orientation. We first point to the fact that the head group is zwitterionic and the two opposite charges in the head group try to lay in the same plane. Another reason for the close proximity of the head group segments to the membrane core is that the hydrophobic segments in the head group can escape some water contacts by laying flat.

The glycerol units are positioned at the core-water interface and do not have an extremely sharp profile. The tails cross the central plane of the bilayer (interdigitation) to some extent. The average position of each segment further towards the tail end is closer to the membrane center. The fluctuations of the position of segments increases towards the chain end as well (not shown). The distribution of the chain ends is also shown in Fig. 1(a). As can be seen the ends have a wide distribution, but the mean position remains on a positive coordinate. Again there is significant interdigitation, but the chains remain on average with all their segments in the same monolayer.

In Fig. 1(b) we give information on the mixed cholesterol-lipid bilayer. In this figure we do not show the details of the lipid molecules. Qualitatively they do not change dramatically. Quantitatively there are changes which we will discuss below in some detail. In Fig. 1(b) we give the total distribution of lipids plus cholesterol which turns out to be very similar to the lipid distribution given in Fig. 1(a). Again the overall density in the core is virtually constant. Also the water distribution is very similar as expected. The overall membrane thickness is not the same in Figs. 1(a) and 1(b), but we will return to this point below. Very surprising is the profile of the lipids and the cholesterol. The lipids have a dip in the center and the cholesterol profile has, consequently, a trian-

gular shape, i.e., the volume fraction of cholesterol increases approximately linearly towards the center of the bilayer. To understand this profile we need to realize that it is the average of many cholesterol molecules, that there are fluctuations of the position of the height in the bilayer as well as orientation of the molecules.

It is known from literature that the electron density profiles (or mass density profiles) of different lipid bilayers appear to have a dip in the center. This feature has been observed, e.g., for 16:0/16:0 PC-cholesterol systems with 0, 4.7, 12.5, 20.3, 29.7, and 50.0 mol % cholesterol (MD simulation) [36]; 16:0/16:0 PC bilayers with 0, 5, 10, 15, 25, and 40 mol % cholesterol (MD simulation) [37]; 16:0/16:0 PC bilayers with 0, 11, and 50 mol % cholesterol (MD simulation) [76]; 14:0/14:0 PC bilayers with 0 and 30 mol % cholesterol (neutron diffraction and MD simulation) [77]; 16:0/16:0 PC bilayers with 0 and 12.5 mol % cholesterol (MD simulation) [78]; 14:0/14:0 PC bilayers with 0, 4, 8, and 40 mol % cholesterol (MD simulation) [79]; 16:0/16:0 PC bilayers with 33.3 and 50 mol % cholesterol (combined Monte Carlo and MD simulation) [80]; 18:0/22:6ω3cis PC bilayer with 25 mol % cholesterol (MD simulation) [81]; 16:0/16:0 PC bilayer mixture with 40 mol % cholesterol; and 12:0/12:0 PC bilayer mixture with 40 mol % cholesterol (MD simulation) [82]. This dip may be caused by a lower mass/electron density of the CH_3 groups compared to CH_2. Indeed, the effective size of a CH_3 is about twice that of a CH_2 group. Such issues cannot easily be accounted for in a lattice model. Indeed the translation of the volume fraction profile to the number/mass/electron density profiles is not trivial.

According to the experimental and computer simulation data the electron (mass) density profiles of cholesterol (for various cholesterol concentrations) are bimodal, with a dip in the center of the bilayer system [36,76–81] (the systems from the simulation works were described above). In particular, it is found by MD [81] that in the 18:0/22:6ω3cis PC-25 mol % cholesterol bilayer system the cholesterol is located primarily in the upper acyl chain region, balancing the tendency for the ring system to occupy the hydrophobic core with the hydroxyl group's need to hydrogen bond to water and/or the polar lipid groups. The position of the cholesterol OH group strongly correlates to that of the lipid carbonyl groups [81]. It is interesting that in the work [82] similar bimodal curve is detected for cholesterol electron density profile in 16:0/16:0 PC-40 mol % cholesterol bilayer, but for the bilayer system with essentially shorter acyl chains, 12:0/12:0 PC, and with 40 mol % cholesterol another picture is observed: the electron density profile of cholesterol has three peaks including a maximum in the bilayer centre. Such a profile can be considered as approximately triangular.

The volume fraction profile of the cholesterol hydroxyl group (O) in Fig. 1(b) has a weak maximum near the glycerol region of the bilayer (hard to see in this figure), but we find significant values also near the center of the bilayer. The profile of the rigid fragment (X) is almost flat in the center of the bilayer. The results do not show the same high correlation between the hydrophilic group of cholesterol and the lipid carbonyl groups as found in MD [81].

The conformations of the flexible moiety of the cholesterol-look-alike (C) are responsible for the central peak. As there are several CH_3 groups in this moiety, it is likely that the corresponding mass density is significantly altered, that is that the mass density is not as high as suggested by the SCF volume fractions.

The orientational order of the rigid part is very high (the order parameter, which will be defined below [see Eq. (5)] is an increasing function of the amount of cholesterol in the bilayer and reaches $S \approx 0.8$ in the present case), which means that most of the chains are nearly perpendicular to the membrane surface. The wide distribution of the O groups proves that the cholesterol has a significant degree of freedom to move in the normal direction as long as it remains in the apolar core. In other words the hydrophilic group on the cholesterol only marginally anchors the cholesterol to the water surface. This is not too surprising considering the huge minority situation this group has within the cholesterol molecule. We note that the distribution of the O group in cholesterol is significantly sharper when the amount of cholesterol is lower.

Apart for the bilayers with short acyl chains, where a significant amount of cholesterol was found in the central region of the bilayer [82], the SCF results seems to be in conflict with experimental and simulation results regarding the z degree of freedom of cholesterol. We mention again that the volume fraction profiles should be translated to the mass density before one can judge the true magnitude of the deviations. Such correction will definitely not lead to the strong bimodal distributions of cholesterol often found in MD. There still are reasons to be cautious regarding the latter simulation results. One should always keep in mind that all-atom MD simulations rarely exceed the ns time window. As the starting configuration in MD simulations typically take the cholesterol evenly distributed over the two halves of the bilayer (with their OH group close to the water phase), and interbilayer crossings of cholesterol molecules is expected to be slow (or effectively prohibited due to the finite size of the system), it may well be that the equilibration of the z positions will not, or not fully take place during the simulations. Major displacements of the cholesterol molecules must result in major conformational changes of a large number of lipid molecules, and significant crossings of cholesterol molecules of the symmetry plane (which should also occur in an equilibrium simulation) may induce huge local pressures because of the finite size of the simulation box. To resolve this issue, it would be of interest to do MD simulations wherein the hydrophilic group of the cholesterol is removed or placed somewhere else in the molecule. Alternatively, we may speculate that the approximations made in the intermolecular and intramolecular excluded volume correlations in the SCF model, or the approximate nature of the cholesterol-look-alikes, has allowed a too high normal mobility of the inclusions. To obtain information on the effects of the molecular architecture, it is natural to study the influence of variations in the structure of the cholesterol-look-alikes in the SCF model.

Here we choose to consider the effects of the length of the rigid fragment n. Our first focus is on some overall characteristics of the bilayer upon the increase of the fraction of cholesterol-look-alikes in the bilayer. In Fig. 2(a) we present the membrane thickness defined by the distance across the

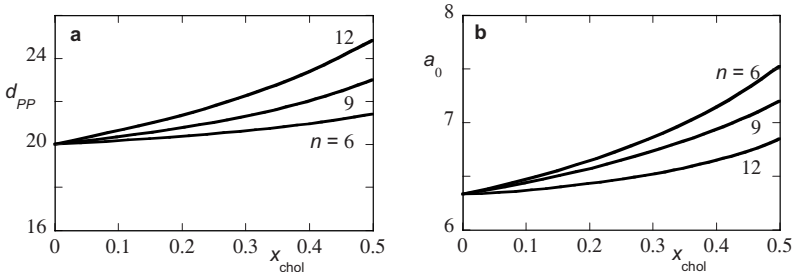

FIG. 2. (a) The phosphate-phosphate distance, a measure for the membrane thickness, units l, as a function of the mole fraction of cholesterol-look-alikes. (b) The area available per PC head group in units $l^2\sqrt{2}$ as a function of the mole fraction of cholesterol-look-alikes. The length of the rigid part $n=6$, 9, and 12 is indicated.

bilayer of the phosphate groups d_{PP}. As expected, inclusions increase the membrane thickness. This is more pronounced for the longer cholesterol-look-alikes and the growth of membrane thickness is slightly stronger than linear. The reason for this nonlinear growth is that the orientational order of the cholesterol molecules increases with increasing n and x.

Indeed, according to MD simulations of 16:0/16:0 PC bilayers with 0, 5, 10, 15, 25, and 40 mol % cholesterol [37], the simulation box height (i.e., the membrane thickness as well) increases with cholesterol concentration. As mentioned in the Introduction, cholesterol can either increase or decrease the width of the bilayer depending on the physical state and chain length of the lipid before the introduction of cholesterol [33]. X-ray diffraction study [33] showed that for saturated PCs containing 12–16 carbons per chain, cholesterol increases the width of the bilayer as it removes the chain tilt from gel state lipids or increases the *trans* conformations of the chains for liquid crystalline lipids (in accordance with Refs. [6–9]).

Also in line with expectations is that the area available per PC head group increases with increasing loading. This is shown in Fig. 2(b). As the shorter cholesterol-look-alike is a better surfactant, it assists with the hydroxyl in the repulsive interactions in the head group region that controls the optimal area per molecule in the self-assembly process. This allows the lipids to pack further apart. The area increase for the long cholesterol is just a weak function of the fraction of cholesterol, except for high loading.

The increase in membrane thickness must have consequences for the conformational properties of the lipid molecules. For example, the tails should have fewer possibilities to cross the center of the bilayer. The average position and the fluctuations of the end segments of the acyl chains are presented in Fig. 3 again as a function of the mole fraction of cholesterol and for the three variants of the cholesterol-look-alikes. The end of the *sn*-1 chain (which is saturated) is known to reach closer to the membrane center ($z=0$) than the end of the longer unsaturated *sn*-2 chain [51]. As shown in Fig. 3(a) the difference is approximately 0.3 nm and this increases somewhat with increasing loading of the bilayer with cholesterol. The mean position of the *sn*-1 chain does not change much. As we will see below the orientational order of the saturated chain increases with increasing mole fraction of cholesterol and this is consistent with the increase in membrane thickness. The average end point of the *sn*-2 chain increases more with increasing loading and this increase follows the increase of thickness of the bilayer.

Previous SCF calculations already showed that the fluctuations of the end of the saturated tail 18:0 exceed those of the unsaturated one [51], whereas in the MD simulations the unsaturated chain 22:6 is fluctuating most [51]. In Fig. 3(b) it is shown that the fluctuations of the end points increase with increasing mole fraction of cholesterol-look-alikes. This is somewhat unexpected from the fact that the orientational order of the lipid tails increase as we will show below. The fluctuations increase more for the longer cholesterol variant than for the shorter one.

One of the experimentally observable quantities is the segment order parameter. This is defined by

$$S(t) = \left\langle \frac{3}{2}\cos^2\alpha(t) - \frac{1}{2} \right\rangle, \tag{5}$$

where $\alpha(t)$ is given by the orientation of the bonds connected to segment t with respect to the bilayer normal. When the two bonds connected to segment t are both pointing in the z direction then $\alpha(t)=0°$, when both bonds are in the x-y plane, that is parallel to the membrane surface $\alpha(t)=90°$, etc. Typically, when the order parameter is close to unity the chains are all in the trans conformation parallel to the membrane normal. When the orientation is random the order parameter is zero and when all chains are parallel to the membrane surface the order parameter is −0.5. In Fig. 4 we present the order parameter for composite membranes with a mole fraction of cholesterol-look-alikes $x=0.4$, together with the unperturbed order parameter profile for the pure bilayer (for reference). The saturated *sn*-1 chain has a smooth order parameter profile. The ranking numbering starts with the car-

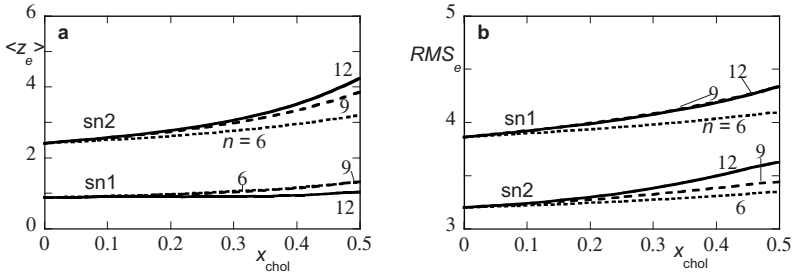

FIG. 3. (a) The average position of the chain end (in units l) and (b) the root mean square position of the chain ends (in units l) for the *sn*-1 and *sn*-2 chains for $n=6$ (dotted line), 9 (dashed line), and 12 (solid line).

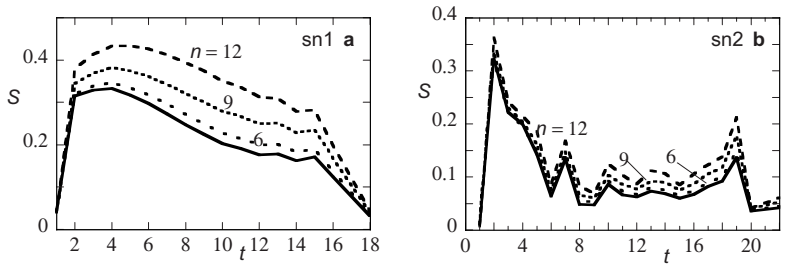

FIG. 4. The segment order parameter as a function of the ranking number of tail segments of (a) the saturated 18:0 *sn*-1 chain and (b) the polyunsaturated 22:6 *sn*-2 chain. The lines connects the data points for convenience. The solid line is the pure bilayer. Other graphs are for a mole fraction of $x=0.4$. The mixed membrane with $n=6$ cholesterol is given by the short dash, the 9-cholesterol is dotted and the 12-cholesterol has a long dashed line.

bon next to the glycerol and ends at the free tail end. Close to the glycerol moiety the orientational order goes through a broad maximum. Near the glycerol backbone the order is relatively low due to the space made available by the *O* sidegroups. Towards the tail ends the order parameter drops gradually. Near the very end the order is almost lost showing that the bond direction becomes isotropic. Admixing cholesterol-look-alikes in the bilayer increases the order homogeneously along the tail. The short variants do this less effectively than the longer ones. This result is consistent with the idea that the rigid part of the cholesterol molecules, especially at relatively high molar ratios, is positioned throughout the hydrophobic region of the bilayer with almost constant probability (see Fig. 1). Each segment along the tails benefits from the oriented rigid parts of the cholesterol-look-alikes. The longer the rigid fragment of the cholesterol molecule the more order it can inflict on the *sn*-1 chain.

Experimental or theoretical order parameter profiles of saturated acyl chains in the presence of cholesterol is known from literature for different lipid bilayers. In all the investigated bilayer systems the cholesterol-induced increase in the order parameters is detected. This effect was observed for 14:0/14:0 PC, 16:0/16:0 PC, 18:0/18:0 PC (^{2}H NMR) [7]; 14:0/14:0 PC (^{2}H NMR) [84] and MD simulation [79]); 16:0/16:0 PC (MD simulation) [36,37,76,82]; 12:0/12:0 PC (MD simulation) [82]; 16:0/16:0 PC (combined Monte Carlo and MD simulation) [80,83]; 18:0/22:6ω3cis PC (MD simulation) [81]; mixed membrane of 18:0/18:1 PC–18:0/18:1 phosphatidylethanolamine–(PE)–18:0/18:1 phosphatidylserine (PS), and membrane of 18:0/22:6ω3cis PC–18:0/22:6ω3*cis* PE–18:0/22:6ω3cis (^{2}H NMR and two-dimensional nuclear Overhauser enhancement ^{1}H NMR spectroscopy with magic angle spinning) [85]; 16:0/22:6ω3cis, 16:0/18:1ω9cis PE (solid-state ^{2}H NMR spectroscopy and low- and wide-angle x-ray diffraction) [86].

In particular, for 16:0/16:0 PC the order parameters grow significantly with an increasing cholesterol content [36]. For pure 16:0/16:0 PC and low cholesterol concentrations, the order parameter profiles in MD simulations show a plateau for small and intermediate values of t (where t is the number of methylene group in the chain) and decay near the center of the bilayer. When the cholesterol content increases, the plateau disappears, and there is a clear maximum at intermediate t. In other words, cholesterol in the simulated bilayers increases the order inhomogeneously (non uniform) along the tail. The ordering effect of cholesterol is most pronounced for $t\sim 6-10$ and quite modest for segments near the phospholipid headgroups and bilayer center (i.e., at the ends of the chain) [36,37]. This is due to the position of the cholesterol ring system in the bilayer along the bilayer normal [76]: the largest ordering occurs for segments at roughly the same depth as the ring system. As a result, with 29.7% cholesterol in 16:0/16:0 PC, the order parameters for $t\sim 6-10$ are increased roughly by a factor of 2 [36]; the same behavior is detected for both *sn*-1 and *sn*-2 16:0-chains in Ref. [83], for 18:0 chain in polyunsaturated 18:0/22:6ω3cis PC bilayer [81]: the effect on the order parameters occurs primarily in the upper half of the 18:0 acyl chain (consistent with the most likely location of the cholesterol molecule). According to Ref. [7] the order parameter in 16:0/16:0 PC with 50 mol % cholesterol for intermediate t was increased by a factor of 2.65. The cholesterol-induced increase in order of the 18:0 chain in the work [85] is two-fold larger in monounsaturated (18:0/18:1ω9*cis*) than in polyunsaturated (18:0/22:6ω3cis) lipids, and the order of both saturated and polyunsaturated hydrocarbon chains increases. The addition of cholesterol (50 mol %) to both 16:0/22:6ω3*cis* PE and 16:0/18:1ω9*cis* PE phospholipids [86] results in an increase in order parameter for each carbon position in the 16:0 chain, but the effect is more pronounced in the plateau region of almost uniform order in the upper part of the acyl chain 16:0 toward the surface of the bilayer [86].

Thus, the SCF results are, in principle, in line with available experimental and theoretical order parameter profiles. Some difference is observed in the degree of uniformity of the order parameter increase along the acyl chain. Yet this difference is consistent with the differences predicted for the degree of freedom of moving along the z coordinate.

The order parameters differs considerably for the *sn*-2 chain. In Fig. 4(b) it is shown that double bonds of the unsaturated chain (there are 6 of them in the *sn*-2 chain), very quickly destroys the orientational order in the chain and the cholesterol molecule is hardly able to improve the situation, albeit that as in the *sn*-1 chain the longer the rigid body the more order it does generate in the *sn*-2 chain. Apparently the disrupting effect of the double bonds is not easily repaired by a rigid body.

To our knowledge, the order parameter profiles for polyunsaturated acyl chains in the lipid/cholesterol bilayer sys-

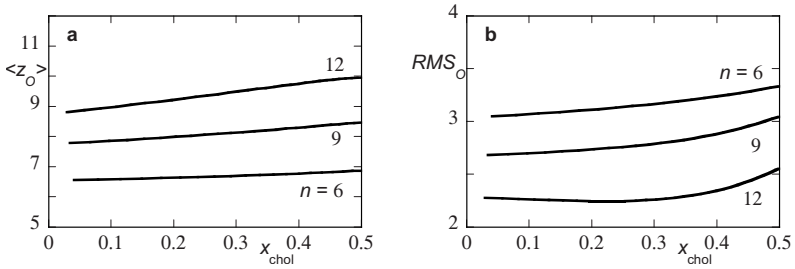

FIG. 5. (a) Average position of the *O* group in the cholesterol-look-alike (in units *l*) and (b) the root-mean-square value for the *O* distribution (in units *l*) as a function of the fraction of the cholesterol-look-alike for three variants of the rigid length of the cholesterol-look-alike molecule as indicated.

tems are not available in literature. The order parameter profiles for polyunsaturated chains in pure lipid monolayers and bilayers were calculated by MD in Refs. [50,51,87–93] and measured experimentally [92] by NMR. The obtained profiles for 22:6ω3*cis* chain in pure lipid bilayers are similar to that of the SCF presented in Fig. 4(b).

Nevertheless, the influence of cholesterol on the order parameter profile of polyunsaturated acyl chain in the lipid bilayer was investigated in MD simulations of 18:0/22:6ω3*cis* PC bilayer with 40 mol % cholesterol. According to these MD simulations the cholesterol molecules do have a detectable influence on the order parameter profile of polyunsaturated chain 22:6ω3*cis*, but in a less degree than on the saturated chain 18:0.

We now shift our attention to the properties of the inclusion molecule in the tensionless bilayers. In Fig. 5 the average position and the fluctuations of the hydrophilic group in the cholesterol-look-alike molecule is presented again for three variants of the rigid backbone length. As shown in Fig. 5(a) the average position is not a very strong function of the loading of the bilayer with the cholesterol-look-alikes, and the *O* shifts further from the center of the bilayer with increasing size of the rigid fragment. The fluctuations have the opposite trend. The further the *O* is from the center the smaller are the fluctuations. The fluctuations remain small for the $n=12$ variant, whereas it is rather high for the smaller ones. The qualitative explanation of these trends is clear. The longer variant is better aligned with the normal and due to its size the *O* must remain on the outside of the bilayer. The average *O* position is at a large coordinate and the fluctuations are small. The reverse is the case for the smallest variant.

Some of our arguments used above rely heavily on the fact that the inclusion molecule is oriented perpendicular to the membrane surface. As is shown in Fig. 6 the order parameter of the rigid fragment is a strong function of the length of the rigid part and only a minor function of the loading of inclusions in the bilayer. Obviously, the order increases with increasing length of the rigid part in the cholesterol-look-alike. Order parameters around 0.8 are very high and one can view these molecules to be in the normal direction to a good approximation. This is in line with above mentioned works and, in particular, with the conclusion made in Ref. [77]: the use of neutron diffraction and proton-deuterium contrast methods as well as molecular dynamics calculations demonstrated that the rigid inclusion is well embedded in the membrane and occupies a vertical location which favors a hydrogen-bonding interaction between its OH group and the phospholipid fatty acyl chain esters. The orientation of cholesterol was measured by solid state ^{2}H NMR in unsaturated 18:0/18:1ω9*cis* PC bilayer and polyunsaturated bilayers of 18:0/20:4ω6*cis* PC and 18:0/22:6ω3*cis* PC as well [24]. This orientation was shown to be almost parallel to the bilayer normal, it is characterized by the tilt angle ~16° with the normal. For dipolyunsaturated 20:4ω6*cis*/20:4ω6*cis* PC bilayer this tilt angle was obtained to be ~22° [24]. A similar result was obtained for cholesterol orientation in 18:0/22:6ω3*cis* PC and 22:6ω3*cis*/22:6ω3*cis* PC bilayers using low- and wide-angle x-ray diffraction [25]: at 20 °C the tilt angle in 22:6ω3*cis*/22:6ω3*cis* PC–50 mol % cholesterol system is ~24°, in 18:0/22:6ω3*cis* PC–50 mol % cholesterol system it is ~17°. For 16:0/16:0 PC bilayers with 33.3 and 50 mol % cholesterol studied by combined Monte Carlo and MD simulation [80] the most probable cholesterol tilt angle is equal to ~12° and ~10°, respectively. In the MD simulations of 16:0/16:0 PC with 50 and 11 % cholesterol concentrations [76] values for the cholesterol tilt angle of ~11° and ~20°, respectively, are reported. According to Ref. [37] the average tilt of the cholesterol ring system in the simulated (by MD) 16:0/16:0 PC bilayer drops from 42° at 5% cholesterol down to ~28° at 40%.

The order parameter *S* for cholesterol in 18:0/22:6ω3*cis* PC–10 mol % cholesterol bilayer was shown to be ~0.68 at 20 °C and ~0.65 at 30 °C. In the bilayer of 18:0/22:6ω3*cis* PC–50 mol % cholesterol the order parameter of cholesterol is ~0.77 at 20 °C and ~0.75 at 30 °C [25]. SCF results shown in Fig. 6 are in good agreement with these data.

The smaller variant is somewhat less ordered, but still it is better aligned to the membrane normal than the lipid molecules. The alignment must be attributed to the fact that there is orientational order in the densely packed system and not as much to the hydroxyl unit in the molecule.

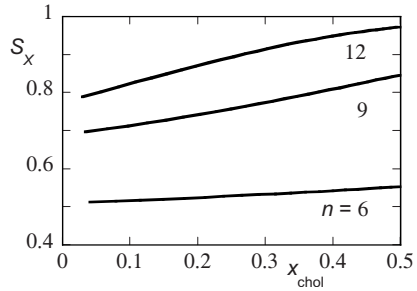

FIG. 6. The order parameter of the rigid fragment of the cholesterol-look-alike molecule as a function of the mole fraction of cholesterol-look-alike in the bilayer for different cholesterol-look-alike variants with the length of the rigid fragment as indicated.

IV. DISCUSSION

The SCF modeling of pure bilayers has been shown to be much better than one could expect *a priori*. Apparently, the theory behaves rather well for densely packed layers wherein the actual surroundings of each molecule does not deviate much from the average surroundings that is found iteratively in the SCF method. Whether the theory is also reasonably accurate in mixed bilayers where the cholesterol-like molecules are admixed with the bilayer lipids is still not obvious. When the interactions between the additives and the lipid molecules are not ideal one should anticipate some lateral clustering of cholesterol, and the present mean-field approximation can not deal with this. In many biological membranes the loading of membranes with cholesterol is very high [44]. This suggests that the mixing is not far from the ideal case. As a result we may anticipate that the clustering is weak and that a mean-field theory should once again be rather accurate. We note, however, that significant amounts of cholesterol mixed with membranes composed of several types of lipids (mixtures of saturated and unsaturated) may not necessarily remain distributed homogeneously. The evidence is mounting that in these systems there can be an inhomogeneous lipid distribution along the bilayer. Regions rich in cholesterol and saturated lipids float similar to rafts in a sea of unsaturated lipids. This means that there can be cholesterol rich domains at some part of the bilayer and region with much less cholesterol in other regions. Recent self-consistent field modeling (significantly different from ours) has given first evidence for such coexistence [94] and the thermodynamic stability of rafts. In this SCF model the molecular structure of the hydrophobic parts of the lipids and the cholesterol were accurately accounted for. However, there were still positional constraints on the molecules (effectively, only the apolar regions of the mixed bilayers were considered). In our SCF theory we do not need to introduce such constraints and therefore it may be useful to use our approach for the problem of rafts formation, i.e., for three-component systems.

One may argue that the present model of the cholesterol-look-alikes is not very realistic. Indeed, the implemented structure has only the main features that correspond to the real cholesterol molecules. The ring structure which is present in the cholesterol molecule is represented by a string of segments that are artificially modeled close to rodlike. The volume of this part is therefore significantly underestimated. Moreover we did not implement the methyl side groups in the rigid part of the molecule. From the analysis in which the length of the rigid part of the cholesterol-look-alikes was varied, we may conclude that the SCF theory indicates that the size of this moiety is important for the response of the surrounding lipids to the cholesterol molecules. The $n=9$ variant is to our opinion close to the length of the real cholesterol molecule and therefore we suggest that the results obtained for this molecule are the most relevant.

The flexible moiety of the cholesterol molecule resembles that in the look-alikes. This part of the molecule is located around the center of the bilayer and the average profile causes the overall profile of the cholesterol to increase almost linearly towards the center of the bilayer. If the cholesterol molecules would not be able to sample conformations in the z direction, and when the O would have been perfectly anchored to the water interface, we would have expected that the overall profile of the cholesterol molecules would have a dip rather than a peak in the center of the bilayer. Note, that the dip in electron density and/or mass density profiles (as found in experiments / MD simulations) is in part due to a relatively high content of CH_3 groups in the central region of the bilayer. This effect is not accounted for in the SCF model. Considering the fact that the glycerol moiety in the bilayer also has some spread in the z direction, we should anticipate that cholesterol has significant z-position fluctuations in the bilayer. These fluctuations are only damped by the "anchoring" of a single O near the glycerol moieties of the lipids. Unless we have severely underestimated the penalty for the desolvatation of this group we must accept a reasonable freedom for the cholesterol to vary its average z position. When this could be established, e.g., by experiments of other computer simulations, this may have interesting implications.

One of the significant predictions of our calculations is that the area per molecule available per PC head group slightly increases with loading of the bilayer with cholesterol. If the lateral mobility of the lipids in the bilayer is limited by some "friction" in the head group region, we may anticipate a larger lateral mobility of the lipids. A larger mobility of the lipids may also expected from a higher orientational order. When the lipid tails have more order they are also less likely entangled with neighbors. The increased packing density may lead to a decreased mobility (as in the gel phase). Finally, the mobility may increase because the cholesterol tends to push the lipids of the two monolayers of the bilayers apart such that there is somewhat less lipid interdigitation. However, when the cholesterol molecules can cross the membrane center (as indicated by the SCF results), we should expect some mechanical coupling of the two halves of the bilayer which leads to a higher friction and a reduction in mobility. This last effect was reported some time ago as a conclusion from quasielastic neutron scattering experiments for dipalmitoylphosphatidylcholine multilayers loaded with cholesterol [95].

V. SUMMARY

A detailed self-consistent field theory has been used to probe the effect of cholesterol-like molecules in densely packed layers of lipids in the bilayer configuration. Cholesterol increases the membrane thickness, increases the area per PC lipid molecule, increases the order in the lipid tails and somewhat decouples the two monolayers in the bilayer. The overall volume fraction profile of the cholesterol-look-alike across the tensionless bilayers reveals a clear maximum in the center of the bilayer. This maximum was attributed to the profile of the flexible chain fragment because the rigid moiety has a rather flat distribution across the bilayer. If we believe our SCF results, we must conclude that the oxygen in the cholesterol molecule is not a very strong anchoring unit to fully fix the molecule to the water interface. As a result one should anticipate that the cholesterol molecule, which is

well aligned with the membrane normal, has significant fluctuations in the normal direction throughout the hydrophobic cores. We have speculated that the dip seen in the mass-density profiles for the cholesterol in MD simulations can be due to the limited simulation time. Another factor that contributes to the dip in simulations and in experiments is that CH_3 groups contribute relatively little to the mass and electron density. The "translation" of the volume fractions (from SCF) to the mass density (in MD) is needed to estimate the true discrepancy between the results. For the majority of predictions we find good correspondence between SCF and experimental and simulation data. This is significant considering the fact that SCF is many orders of magnitude cheaper in CPU time than MD.

ACKNOWLEDGMENTS

This work has been supported by NWO (Dutch-Russian grant "Computational approaches for multiscale modeling in self-organizing polymer and lipid systems"), Russian Foundation for Basic Research (Grant No. 06-03-32211).

[1] H. Ohvo-Rekilä, B. Ramstedt, P. Leppimäki, and J. P. Slotte, Prog. Lipid Res. **41**, 66 (2002).
[2] D. Bach and E. Wachtel, Biochim. Biophys. Acta **1610**, 187 (2003).
[3] H. M. McConnell and A Radhakrishnan, Biochim. Biophys. Acta **1610**, 159 (2003).
[4] H. L. Scott, Curr. Opin. Struct. Biol. **12**, 495 (2002).
[5] J. R. Silvius, Biochim. Biophys. Acta **1610**, 174 (2003).
[6] B. W. Stockton and I. C. P. Smith, Chem. Phys. Lipids **17**, 251 (1976).
[7] M. B. Sankaram and T. E. Thompson, Biochemistry **29**, 10676 (1990).
[8] M. A. Davies, H. F. Schuster, J. W. Brauner, and R. Mendelsohn, Biochemistry **29**, 4368 (1990).
[9] D. Kurad, G. Jeschke, and D. Marsh, Biophys. J. **86**, 264 (2004).
[10] E. J. Shimshick and N. M. McConnell, Biochem. Biophys. Res. Commun. **53**, 446 (1973).
[11] B. De Kruijff, R. A. Demel, A. J. Slotboom, L. L. M. Van Deenen, and A. F. Rosenthal, Biochim. Biophys. Acta **307**, 1 (1973).
[12] J. Ulmius, H. W. Wennerström, G. Lindblom, and G. Arvidson, Biochim. Biophys. Acta **389**, 197 (1975).
[13] P. L. Yeagle, Biochim. Biophys. Acta **822**, 267 (1985).
[14] J. H. Ipsen, G. Kalström, O. G. Mouritsen, H. W. Wennerström, and M. J. Zuckermann, Biochim. Biophys. Acta **905**, 162 (1987).
[15] M. R. Vist and J. H. Davis, Biochemistry **29**, 451 (1990).
[16] P. F. F. Almeida, W. L. C. Vaz, and T. E. Thompson, Biochemistry **31**, 6739 (1992).
[17] R. N. A. H. Lewis and R. N. McElhaney, in *The Structure of Biological Membranes*, edited by P. L. Yeagle (CRC, Boca Raton, 1992), pp. 73–156.
[18] P. R. Maulik and G. G. Shipley, Biophys. J. **70**, 2256 (1996).
[19] P. A. Edwards and R. Davis, in *Biochemistry of Lipids, Lipoproteins and Membranes*, edited by D. E. Vance and J. E. Vance (Elsevier, Amsterdam, 1996), pp. 341–362.
[20] E. K. Tiburu, P. C. Dave, and G. A. Lorigan, Magn. Reson. Chem. **42**, 132 (2004).
[21] R. Bittman, in *Cholesterol: Its Functions and Metabolism in Biology and Medicine*, edited by R. Bittman (Plenum Press, New York, 1997), pp. 145–172.
[22] T. P. W. McMullen, R. N. A. H. Lewis, and R. N. McElhaney, Biochemistry **32**, 516 (1993).
[23] J. Villalain, Eur. J. Biochem. **241**, 586 (1996).
[24] M. R. Brzustowicz, W. Stillwell, and S. R. Wassall, FEBS Lett. **451**, 197 (1999).
[25] M. R. Brzustowicz, V. Cherezov, M. Zerouga, W. Stillwell, and S. R. Wassall, Biochemistry **41**, 12509 (2002).
[26] C. Chachaty, D. Rainteau, C. Tessier, P. J. Quinn, and C. Wolf, Biophys. J. **88**, 4032 (2005).
[27] W. Guo, V. Kurze, T. Huber, N. H. Afdhal, K. Beyer, and J. A. Hamilton, Biophys. J. **83**, 1465 (2002).
[28] W. Guo and J. A. Hamilton, Biochemistry **34**, 14174 (1995).
[29] T. J. McIntosh, S. A. Simon, D. Needham, and C. H. Huang, Biochemistry **31**, 2012 (1992).
[30] J. B. Finean, Chem. Phys. Lipids **54**, 147 (1990).
[31] A. Parker, K. Miles, K. H. Cheng, and J. Huang, Biophys. J. **86**, 1532 (2004).
[32] D. Needham and R. S. Nunn, Biophys. J. **58**, 997 (1990).
[33] T. J. McIntosh, Biochim. Biophys. Acta **513**, 43 (1978).
[34] J. Lemmich, K. Mortensen, J. H. Ipsen, T. Hønger, R. Bauer, and O. G. Mouritsen, Eur. Biophys. J. **25**, 293 (1997).
[35] O. Edholm and J. F. Nagle, Biophys. J. **89**, 1827 (2005).
[36] E. Falck, M. Patra, M. Karttunen, M. T. Hyvönen, and I. Vattulainen, Biophys. J. **87**, 1076 (2004).
[37] C. Hofsäb, E. Lindahl, and O. Edholm, Biophys. J. **84**, 2192 (2003).
[38] A. Radhakrishnan and H. M. McConnell, Proc. Natl. Acad. Sci. U.S.A. **102**, 12662 (2005).
[39] H. M. McConnell and A. Radhakrishnan, Biochim. Biophys. Acta **1610**, 159 (2003).
[40] D. Scherfeld, N. Kahya, and P. Schwille, Biophys. J. **5**, 3758 (2003).
[41] N. Kahya, D. Scherfeld, and P. Schwille, Chem. Phys. Lipids **135**, 169 (2005).
[42] T. P. Trouard, A. A. Nevzorov, T. M. Alam, C. Job, J. Zajicek, and M. F. Brown, J. Chem. Phys. **110**, 8802 (1999).
[43] C. L. Guernevė and M. Auger, Biophys. J. **68**, 1952 (1995).
[44] J. H. Davis, in *Cholesterol in Membrane Models*, edited by L. Finegold (CRC Press, Boca Raton, 1993), pp. 67–136.
[45] M. P. Allen and D. J. Tildesley, *Computer Simulation of Liquids* (Clarendon, Oxford, 1987), p. 385.
[46] D. Frenkel and B. Smit, *Understanding Molecular Simulation. From Algorithms to Applications* (Academic Press, San Diego, 1996), p. 443.
[47] R. J. Sadus, *Molecular Simulations of Fluids. Theory, Algorithms and Object-Orientation* (Elsevier, Amsterdam, 1999),

p. 523.
[48] S. E. Feller, in *Lipid Bilayers. Structure and Interactions*, edited by J. Katsaras and T. Gutberlet (Springer-Verlag, Berlin, 2001), pp. 89–107.
[49] L. Saiz and M. L. Klein, Acc. Chem. Res. **35**, 482 (2002).
[50] A. L. Rabinovich, P. O. Ripatti, N. K. Balabaev, and F. A. M. Leermakers, Proc. SPIE **4627**, 141 (2002).
[51] A. L. Rabinovich, P. O. Ripatti, N. K. Balabaev, and F. A. M. Leermakers, Phys. Rev. E **67**, 011909 (2003).
[52] F. A. M. Leermakers, A. L. Rabinovich, and N. K. Balabaev, Phys. Rev. E **67**, 011910 (2003).
[53] R. C. Valentine and D. L. Valentine, Prog. Lipid Res. **43**, 383 (2004).
[54] A. L. Rabinovich, Usp. Sovrem. Biol. **114**, 581 (1994).
[55] W. Stillwell and S. R. Wassall, Chem. Phys. Lipids **126**, 1 (2003).
[56] S. E. Feller and K. Gawrisch, Curr. Opin. Struct. Biol. **15**, 416 (2005).
[57] R. A. Gibson, W. Chen, and M. Makrides, Lipids **36**, 873 (2001).
[58] A. Lapillonne and S. E. Carlson, Lipids **36**, 901 (2001).
[59] P. C. Calder, Lipids **36**, 1007 (2001).
[60] K. Gawrisch, N. V. Eldho, and L. L. Holte, Lipids **38**, 445 (2003).
[61] M. T. Nakamura, H. P. Cho, J. Xu, Z. Tang, and S. D. Clarke, Lipids **36**, 961 (2001).
[62] S. R. Wassall, M. R. Brzustowicz, S. R. Shaikh, V. Cherezov, M. Caffrey, and W. Stillwell, Chem. Phys. Lipids **132**, 79 (2004).
[63] F. A. M. Leermakers, J. M. H. M. Scheutjens, and J. Lyklema, Biophys. Chem. **18**, 353 (1983).
[64] F. A. M. Leermakers and J. M. H. M. Scheutjens, J. Chem. Phys. **89**, 3264 (1988).
[65] F. A. M. Leermakers and J. M. H. M. Scheutjens, J. Chem. Phys. **89**, 6912 (1988).
[66] F. A. M. Leermakers, J. M. H. M. Scheutjens, and J. Lyklema, Biochim. Biophys. Acta **1024**, 139 (1990).
[67] F. A. M. Leermakers and J. M. H. M. Scheutjens, J. Colloid Interface Sci. **136**, 231 (1990).
[68] G. J. Fleer, M. A. Cohen Stuart, J. M. H. M. Scheutjens, T. Cosgrove, and B. Vincent, *Polymers at Interfaces* (Chapman and Hall, London, 1993).
[69] L. A. Meijer, F. A. M. Leermakers, and J. Lyklema, J. Chem. Phys. **110**, 6560 (1999).
[70] L. A. Meijer, F. A. M. Leermakers, and J. Lyklema, Recl. Trav. Chim. Pays-Bas **113**, 167 (1994).
[71] M. C. Wiener and S. H. White, Biophys. J. **61**, 434 (1992).
[72] H. Akitsu and T. Nagamori, Biochemistry **30**, 4510 (1991).
[73] G. Büldt, H. U. Gally, A. Seelig, and G. Zaccai, J. Mol. Biol. **134**, 673 (1979).
[74] H. Hauser, I. Pascher, R. H. Pearson, and S. Sundell, Biochim. Biophys. Acta **650**, 21 (1981).
[75] J. Seelig, P. M. MacDonald, and P. G. Scherer, Biochemistry **26**, 7535 (1987).
[76] A. M. Smondyrev and M. L. Berkowitz, Biophys. J. **77**, 2075 (1999).
[77] A. Léonard, C. Escrive, M. Laguerre, E. Pebay-Peyroula, W. Néri, T. Pott, J. Katsaras, and E. J. Dufourc, Langmuir **17**, 2019 (2001).
[78] K. Tu, M. L. Klein, and D. J. Tobias, Biophys. J. **75**, 2147 (1998).
[79] P. Jedlovszky and M. Mezei, J. Phys. Chem. B **107**, 5311 (2003).
[80] S. W. Chiu, E. Jakobsson, and H. L. Scott, J. Chem. Phys. **114**, 5435 (2001).
[81] M. C. Pitman, F. Suits, A. D. MacKerell, S. E. Feller, Jr., Biochemistry **43**, 15318 (2004).
[82] S. A. Pandit, D. Bostick, and M. L. Berkowitz, Biophys. J. **86**, 1345 (2004).
[83] S. W. Chiu, E. Jakobsson, R. J. Mashl, and H. L. Scott, Biophys. J. **83**, 1842 (2002).
[84] J. A. Urbina, S. Pekerar, H.-b. Le, J. Patterson, B. Montez, and E. Oldfield, Biochim. Biophys. Acta **1238**, 163 (1995).
[85] D. Huster, K. Arnold, and K. Gawrisch, Biochemistry **37**, 17299 (1998).
[86] S. R. Shaikh, V. Cherezov, M. Caffrey, W. Stillwell, and S. R. Wassall, Biochemistry **42**, 12028 (2003).
[87] A. L. Rabinovich, P. O. Ripatti, and N. K. Balabaev, Proc. SPIE **4064**, 144 (2000).
[88] A. L. Rabinovich, P. O. Ripatti, and N. K. Balabaev, Zh. Fiz. Khim. **74**, 1990 (2000) [Russ. J. Phys. Chem. **74**, 1809 (2000)].
[89] A. L. Rabinovich and N. K. Balabaev, Proc. SPIE **4348**, 215 (2001).
[90] L. Saiz and M. L. Klein, Biophys. J. **81**, 204 (2001).
[91] S. E. Feller, K. Gawrisch, and A. D. Jr. MacKerell, J. Am. Chem. Soc. **124**, 318 (2002).
[92] T. Huber, K. Rajamoorthi, V. F. Kurze, K. Beyer, and M. F. Brown, J. Am. Chem. Soc. **124**, 298 (2002).
[93] C. Gliss, O. Randel, H. Casalta, E. Sackmann, R. Zom, and T. Bayerl, Biophys. J. **77**, 331 (1999).
[94] R. Elliott, I. Szleifer, and M. Schick, Phys. Rev. Lett. **96**, 098101 (2006).
[95] C. Gliss, O. Randel, H. Casalta, E. Sackmann, R. Zorn, and T. Bayerl, Biophys. J. **77**, 331 (1999).